J. Am. Chem. Soc. 1995, 117, 11584−11585

Molecular "Trigger" for Radiationless Deactivation of Photoexcited Conjugated Hydrocarbons

Paolo Celani,[†] Marco Garavelli,[†] Stefano Ottani,[‡]
Fernando Bernardi,[†] Michael A. Robb,[*,§] and
Massimo Olivucci[*,†]

Dipartimento di Chimica "G. Ciamician" dell'
Università di Bologna, Via Selmi 2, 40126 Bologna, Italy
Centro di Studio per la Fisica delle
Macromolecole del CNR, Bologna, Italy
King's College London, London, U.K.

Received June 16, 1995

Conjugated hydrocarbons are the subject of intensive investigation because of light-induced effects involving radiationless return to the ground state. These include the photoconversion of biomolecules and photochromic materials,[1,2] photoconductivity, and non-linear-optical properties.[3] High-resolution fluorescence excitation spectra are being used to elucidate the mechanism of these phenomena in short polyenes and indicate that there is a small threshold energy to ultrafast radiationless decay.[4,5] Here we use state-of-the-art *ab-initio* computations to demonstrate that the general mechanism which "triggers" the decay is a displacement of the electronically excited equilibrium structure toward a "critical" configuration where the excited and ground states cross at a conical intersection.[6,7] The molecular geometry at the point of decay shows, invariably, a sharp "kink" located at a $-(CH)_3-$ segment in the middle of the molecule.

More than 25 years ago Edward Teller suggested that conical intersections may provide a universal decay route from the lower excited states of polyatomics.[6] Independently, both Zimmerman and Michl suggested that conical intersections may have a role to play in photochemical mechanisms.[8,9] More recently, theoretical and computational methods have been used in an attempt to predict or locate the exact molecular structure of conical intersections.[10] In these studies, special attention has been devoted to conjugated molecules because of the importance of photochemical *cis*−*trans* isomerizations in nature. However, only in the last few years it has become possible to investigate conical intersections using unconstrained optimization and reaction path following methods coupled to high-level *ab-initio* computations.[11−14] Recently, we have established that two polyenes, butadiene and *cis*-hexatriene, have low-energy conical intersections between the S_1 and S_0 states.[15,16] These intersections are located at the end of the excited state reaction path (the minimum energy path)[17] on the S_1 potential energy surface, and this decay for *s-trans*-butadiene is illustrated in Figure 1. The conical intersection is reached by twisting about two C−C bonds and decreasing of one of the C−C−C angles. As we shall now discuss, this type of decay route and the "kink" in the carbon backbone associated with the small C−C−C angle are *general* features for conjugated hydrocarbons with formula C_nH_{n+2}.

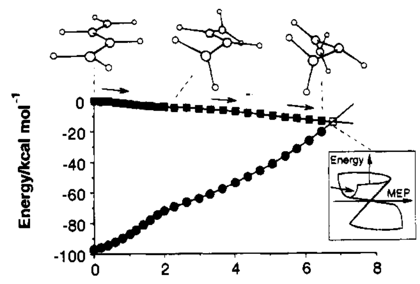

Figure 1. Excited (■) and ground (●) state energy profiles along the minimum energy path (MEP) connecting S_1 butadiene (origin) to a conical intersection (curve crossing). (This data is more accurate than that presented in ref 15 due to the use of an extended basis.) The "ball and stick" structures at the top of the figure illustrate the evolution of the molecular geometry along the path. The C_{2h} symmetry structure at the left-hand side corresponds to planar S_1 butadiene. This structure corresponds not to a minimum but to a local maximum. The asymmetric structure at the right-hand side corresponds to the termination point of the reaction path and is close to the conical intersection. Inset: Schematic representation of the shape ,of the two potential energy surfaces at the conical intersection.[6]

Table 1. Energy Barriers Computed with Second-Order Multireference Møller−Plesset Perturbation Methods

structure (C_nH_{n+2})	energy barrier (kcal mol^{-1}) calcd	energy barrier (kcal mol^{-1}) exptl	structure (C_nH_{n+2})	energy barrier (kcal mol^{-1}) calcd	energy barrier (kcal mol^{-1}) exptl
$n = 3$	0.0[a]	*c, d*	$n = 6$ (*E*/*Z*)[b]	1.5	0.2−0.5[f]
$n = 4$	0.0[a]	*c, e*	$n = 6$ (*c*/*t*)[b]	1.0	~0.0[f]
$n = 5$	8.7		$n = 7$	16.2	
$n = 6$	0.0	0.0−0.3[c,f,g]	$n = 8$	7.6	6.0[h]

[a] For $n = 3, 4$ the reaction path is barrierless. [b] To extend the comparison between experimental and computed values of the energy barriers we have also recomputed the energy barriers for the two *cis*-hexatriene decay paths reported in ref 16. [c] Fluorescence not detected. [d] Reference 25. [e] Reference 26. [f] Reference 4a. [g] Reference 5. [h] Reference 4b.

We now proceed to document the excited state decay path for six ($n = 3, ..., 8$) *all-trans* conjugated hydrocarbons: three polyenes (butadiene, hexatriene, and octatetraene) and three polyene radicals (allyl, pentadienyl, and heptatrienyl). The potential energy surfaces of these molecules have been computed using the *ab-initio* multiconfiguration self-consistent field method with the DZ+d basis set and a complete active space (including all π and π^* orbitals and electrons).[18] The lowest energy excited state reaction paths, connecting the optimized planar S_1 or D_1 equilibrium structures to a conical intersection, via the transition structure at the top of the energy profile, have been computed using the intrinsic reaction co-ordinate method.[19] Computations have been carried out using the methods implemented in the Gaussian92 package.[20] The barrier heights have been corrected for dynamic correlation effects by single-point computations using second-order multireference Møller−Plesset

---

[†] Università di Bologna.

[‡] CNR.

[§] King's College London.

(1) Jacobs, H. J. C. *Pure Appl. Chem.* **1995**, *67*, 63−70.

(2) Heller, H. G.; Elliot, C. C.; Koth, K.; Al-Shihry, S.; Whittall, J. In *Photochemistry and Polymeric Systems*; Kelly, J. M., Mc Ardle, C. B., Maunder, M .J. de F., Eds.; The Royal Society of Chemistry: London, 1993; pp 156−168.

(3) Brédas, J. L.; Adant, C.; Tackx, P.; Persoons, A. *Chem. Rev.* **1994**, *94*, 243−278.

(4) (a) Petek, H.; Bell, A. J.; Christensen, R. L.; Yoshiara, K. *SPIE* **1992**, *1638*, 345−356. (b) Petek, H.; Bell, A. J.; Choi, Y. S.; Yoshiara, K.; Tounge, B. A.; Christensen, R. L. *J. Chem. Phys.* **1993**, *98*, 3777−3794.

(5) Hayden, C. C.; Chandler, D. W. *J. Phys. Chem.* **1995**, *99*, 7897−7903.

(6) Teller, E. *Isr. J. Chem.* **1969**, *7*, 227−235.

(7) Manthe, U.; Koppel, H. *J. Chem. Phys.* **1990**, *93*, 1658−1669.

(8) Zimmerman, H. E. *J. Am. Chem. Soc.* **1966**, *88*, 1566−1567.

(9) Michl, J. *J. Mol. Photochem.* **1972**, 243−255.

(10) (a) Bonacic-Koutecky, V.; Koutecky, J.; Michl, J. *Angew. Chem., Int. Ed. Engl.* **1987**, *26*, 170. (b) Michl, J.; Bonacic-Koutecky, V. *Electronic Aspects of Organic Photochemistry*; Wiley: New York, 1990 and references cited therein.

(11) Heumann, B.; Schinke, R. *J. Chem. Phys.* **1994**, *101*, 7488−7499.

(12) Yarkony, D. R. *J. Am. Chem. Soc.* **1994**, *116*, 11444−11448.

(13) Muller, H.; *et al. Chem. Phys. Lett.* **1992**, *197*, 599−606.

(14) Woywod, C.; Domcke, W.; Sobolewski, A. L.; Werner, H.-J. *J. Chem. Phys.* **1994**, *100*, 1400−1413.

(15) Olivucci, M.; Ragazos, I. N.; Bernardi, F.; Robb, M. A. *J. Am. Chem. Soc.* **1993**, *115*, 3710−3721.

(16) Olivucci, M.; Bernardi, F.; Celani, P.; Ragazos, I. N.; Robb, M. A. *J. Am. Chem. Soc.* **1994**, *116*, 1077−1085.

(17) Truhlar, D. G.; Gordon, M. S. *Science* **1990**, *249*, 491−498.

(18) Roos, B. O. *Adv. Chem. Phys.* **1987**, *69*, 399−446.

(19) Gonzales, C.; Schlegel, H. B. *J. Phys. Chem.* **1990**, *94*, 5523−5527.

(20) Frisch, M. J.; Trucks, G. W.; Head-Gordon, M.; Gill, P. M. W.; Wong, M. W.; Foresman, J. B.; Johnson, B. G.; Schlegel, H. B.; Robb, M. A.; Replogle, E. S.; Gomperts, R.; Andres, J. L.; Raghavachari, K.; Binkley, J. S.; Gonzalez, C.; Martin, R. L.; Fox, D. J.; Defrees, D. J.; Baker, J.; Stewart, J. J. P.; Pople, J. A.; *Gaussian 92*, Revision B; Gaussian, Inc.: Pittsburgh, PA, 1992.

0002-7863/95/1517-11584$09.00/0

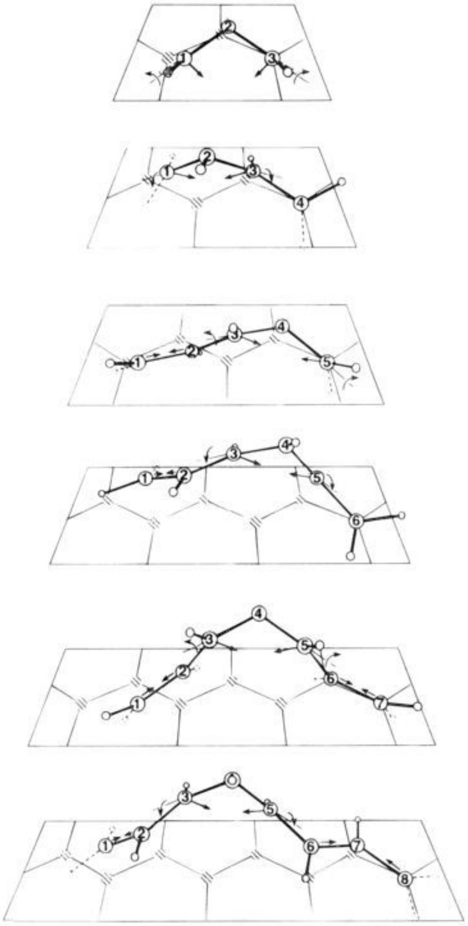

Figure 2. Geometrical structure of the termination point of the excited state reaction path for the hydrocarbons discussed in the text. From top to bottom: allyl radical ($n = 3$), butadiene ($n = 4$), pentadienyl radical ($n = 5$), hexatriene ($n = 6$), heptatrienyl radical ($n = 7$), and octatetraene ($n = 8$). Each structure has the first (C_1), next-to-last, and last carbon centers lying on the plane containing the corresponding excited state equilibrium planar structure (hatched structure). The molecular distortion can be assessed by considering that the last carbon atom in each distorted structure is anchored to the terminal carbon of the underlying planar structure. The arrows indicate the most important distortion modes characterizing each reaction path. The $-(CH_3)-$ kink is located at the $-C_1-C_2-C_3-$ position in butadiene and at the $-C_3-C_4-C_5-$ position in the pentadienyl radical through octatetraene.

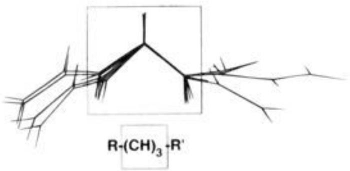

Figure 3. Superimposed $-(CH_3)-$ kinks of all six species. In all cases, the $(CH)_3-R$ bond lengths approach that of a single bond and the R and R′ groups take up the geometries of ground state fragments (e.g., in octatetraene the terminal C_3H_4 group relaxes toward the ground state geometry of an allyl radical).

perturbation methods.[21] The conical intersections have been located by mapping the reaction path until a point of crossing is reached. For $n = 3$ and 4 the existence of a conical intersection at the end of the computed reaction path was also demonstrated by direct search and optimization of the conical intersection point using the methodology reported in ref 22.

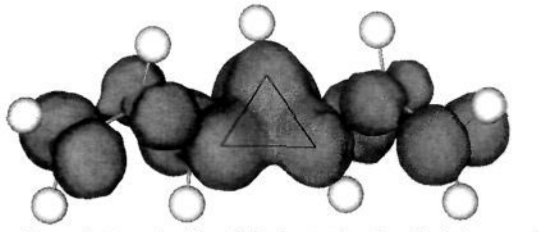

Figure 4. π electron density of the heptatrienyl radical decay point. The $-(CH_3)-$ "kink" is highlighted by the triangle illustrated. The three "fused" lobes and the lack of coalescence of these lobes with the adjacent density regions indicate that the three electrons at the "kink" interact strongly.

In order to "calibrate" the accuracy of our computed results, we give the values of the energy barriers associated with the eight reaction paths (Table 1). The computed barriers heights are slightly larger than the experimental barrier heights and are correct within 1.5 kcal mol^{-1} where comparison with the experimental results is possible. Thus one has confidence that the computed reaction paths correspond to the paths populated at the range of low vibrational excess energies used in the jet experiments.[4,5]

In Figure 2 we show the nature of the geometrical deformation along the reaction path leading to the conical intersection by illustrating the S_1 or D_1 equilibrium planar geometries with the conical intersection geometries superimposed. (The relevant fully optimized geometrical parameters are available as supporting information.) While the initial electronic excitation of conjugated chains is not localized,[23] the subsequent evolution of these structures toward the conical intersection is associated with a localization of the excitation onto an isolated "kinked" $-(CH)_3-$ segment in which the C$-$C$-$C angle ranges from 98° to 108°. In Figure 3 we have superimposed the $-(CH)_3-$ units of all six species. Clearly the $-(CH)_3-$ kink is a general feature. The origin of this feature can be understood by comparison with H_3, where any equilateral triangle configuration corresponds to a point on the D_0/D_1 conical intersection in which the three H electrons have identical pairwise interactions.[24] As shown in Figure 4, the same effect results in the case of conjugated hydrocarbons (see ref 10b for related work on H_4). In the example shown (heptatrienyl radical), the π-electron density is localized along the three equivalent pairwise interactions (i.e., along the lines of the triangle illustrated) of the $-(CH)_3-$ kink.

In conclusion, our computations demonstrate that the molecular mechanism for radiationless decay for six conjugated hydrocarbons is the same. In photochemistry, the conical intersection geometry provides the starting point of the ground state branch of the reaction path. The highly twisted $-(CH)_3-$ structure must therefore play a role in the process of *cis*$-$*trans* isomerization.[16] The computed pathways rigorously describe the evolution of "cold" S_1 polyene molecules as those probed by the jet experiments.[4,5] However, the S_1 motion, when the system is prepared in the S_2 spectroscopic state, may be affected by the initial $S_2 \rightarrow S_1$ relaxation dynamics.

Acknowledgment. This research has been supported by the SERC (U.K.) under Grants GR/J25123 and GR/H58070 and by the CINECA (Italy) under the Grant 92-2-103-2.

Supporting Information Available: Bond lengths, bond angles, and torsional angles (3 pages). This material is contained in many libraries on microfiche, immediately follows this article in the microfilm version of the journal, can be ordered from the ACS, and can be downloaded from the Internet; see any current masthead page for ordering information and Internet access instructions.

JA951976S

---

(21) Serrano-Andrés, L.; Merchán, M.; Nebot-Gil, I.; Lindh, R.; Roos, B. O. *J. Chem. Phys.* **1993**, *93*, 3151−3162. *MOLCAS*, Version 2, Andersson, K., Blomberg, M. R. A., Fülscher, M., Kellö, V., Lindh, R., Malqvist, P.-A., Noga, J., Olsen, J., Roos, B. O., Sadlej, A. J., Siegbahn, P. E. M., Urban, M., Widmark, P. O.; University of Lund, Sweden, 1991.

(22) (a) Ragazos, I. N.; Robb, M. A.; Bernardi, F.; Olivucci, M. *Chem. Phys. Lett.* **1992**, *197*, 217−223. (b) Bearpark, M. J.; Robb, M. A.; Schlegel, H. B. *Chem. Phys. Lett.* **1994**, *223*, 269−274.

(23) Orlandi, G.; Zerbetto, F.; Zgierski, M. Z. *Chem. Rev.* **1991**, *91*, 867−891.

(24) Mead, C. A.; Truhlar, D. G. *J. Chem. Phys.* **1979**, *70*, 2284−296.

(25) Ashfold, M. N. R.; Clement, S. G.; Howe, J. D.; Western, C. M. *J. Chem. Soc., Faraday Trans.* **1993**, *89*, 1153−1172.

(26) Vaida, V. *Acc. Chem. Res.* **1986**, *19*, 114−120.